FEEDBACK LINEARIZATION CONTROL FOR ACTIVE FILTERS

MARCOS B. KETZER, CURSINO B. JACOBINA*

* *Universidade Federal de Campina Grande - UFCG*
Departamento de Engenharia Elétrica - DEE
Campina Grande, Paraíba, Brasil

Email: `marcos.ketzer@ee.ufcg.edu.br, jacobina@dee.ufcg.edu.br`

Abstract— This paper presents the application of the feedback linearization theory to a three-phase shunt active filter. The solution is performed in a synchronous reference frame, dealing with multivariable aspects of system. The proposed control ensures a proper operation of active filter, allowing to achieve high power factor of the grid independent of constants obtained by operation points. Experimental results obtained from a prototype are presented in order to validate the proposed strategy, covering the analysis from stationary and transient responses.

Keywords— Feedback Linearization, Nonlinear Control, Active Filters, Nonlinear Dynamics

Resumo— Este trabalho apresenta a aplicação da teoria feedback linearization em um filtro ativo trifásico. A solução é realizada num eixo de referências síncronas, tratando os aspectos multivariaveis do sistema. O controle proposto garante uma operação satisfatoria do filtro ativo, permitindo alcançar alto fator de potência na rede independentemente das constantes obtidas pelos pontos de operação. Resultados experimentais obtidos em laboratório a partir de um protótipo do conversor são apresentados, abordando a análise em regime e transitória.

Palavras-chave— Feedback Linearization, Controle Não-Linear, Filtros Ativos, Dinâmica Não-Linear

1 Introduction

It is well known control strategy plays the most significant role in Active Power Filters (APF). It is the control strategy which decides the behavior and effectiveness of the compensation (Khadkikar, 2012). Shunt Active Filter (SAF), a specific type of APF, can effectively compensate the harmonic current of nonlinear loads (Cavini et al., 2004), injecting the detected currents distortions with reverse polarity, so getting its cancellation. Thus, several control strategies have been developed for this topology (Caceres et al., 2010; Buso et al., 1998).

However, models of static converters are nonlinear and multivariable, and use of linear techniques of compensation is not adequate. The main nonlinear control strategies applied to active filters are the sliding mode control and feedback linearization. Sliding mode control have some drawbacks, such as excitation of high frequency components, which implies in a lower efficiency. On the other hand, feedback linearization theory have been utilized successfully in several studies (Rahmani et al., 2010; Mendalek et al., 2001; Jiang and Xiang, 2012; Cavini et al., 2004), and appears as one of the best alternatives compatible with the application.

In addition to aspects of performance and robustness, in the control project it is needed to consider the physical aspects of its realization. In this context, for digital implementations, are recognized mainly two aspects: computability and sensing. While the problem of computability has become less aggravating, since since there is a continuous increase in the availability of devices with high processing capability at low cost, reducing the number of sensors, on the other hand, bring to implementation obvious advantages, such as removing offsets and noise related to sensors, absence of resolution limitations of analog converters and smaller number of simultaneous samples. As sensing circuit is reduced, its development becomes simpler in hardware level.

One of the most discussed sensorless techniques applied in rectifiers and active filters is the voltage oriented control (VOC). The strategy consists in the elimination of the grid voltage sensors and estimation of synchronization angle for subsequent coordinate transformation and control of the states of the converter. The estimation can be performed by the voltage drop across the inductor (Kennel and Szczupak, 2005; Hansen et al., 2000), instantaneous power (Noguchi et al., 1998), predictors (Wojciechowski, 2005), state observers (Agirman and Blasko, 2003; Yu and peng Tang, 2008) and virtual flux (Malinowski, 2001). The last strategy is attractive because instead of calculating the derivative of the current is calculated the integral, rejecting high frequency noise.

This paper presents a strategy without grid voltage sensors based on virtual flux oriented control (VFOC), which was presented in (Malinowski, 2001) for three-phase rectifiers. As the model in the synchronous reference frame is nonlinear and multivariable, it is proposed compensation using the feedback linearization theory. Such approach allows to improve the control response by eliminating dependence on operating points, obtained in linearized models, and eliminating the interactions between control loops. Considering that the system has two control inputs and three outputs, the control is arranged in cascade form. The equivalent linear systems are regulated by the proportional, integral and derivative (PID) compensator. At the end of the paper is presented the simulation and experimental results obtained from a laboratory prototype.

2 Development

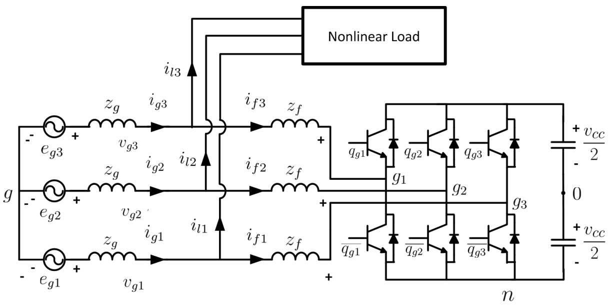

Figure 1: Three-phase three-line active power filter circuit.

Fig 1. Shows a three-phase three-wire active power filter (APF), where z_g is the grid impedance, z_f is the filter impedance (equivalent inductor and resistor), e_{gk} are the voltages of the grid ($k = 1, 2, 3$), v_{cc} is the DC bus voltage. The pole voltages are obtained by

$$v_{gk0} = (2q_k - 1)\frac{v_{cc}}{2} \qquad (k = 1, 2, 3) \tag{1}$$

where q_k is the switch state ($q_k = 1 \rightarrow$ switch closed and $q_k = 0 \rightarrow$ switch open). From Fig. 1 it is obtained

$$e_{gk} = v_{gk} + z_g i_{gk} + z_f i_{fk} \qquad (k = 1, 2, 3) \tag{2}$$

where

$$v_{gk0} = v_{gk} + v_{g0} \qquad (k = 1, 2, 3) \tag{3}$$

$$\sum_{k=1}^{3} v_{gk} = 0 \tag{4}$$

$$v_{g0} = \frac{1}{3}\sum_{k=1}^{3} v_{gk0} \tag{5}$$

where v_{g0} is known as homopolar voltage, which does not induce current in the network. Thus, the homopolar voltage is a degree of freedom and con be used to improve the efficiency of the converter. This paper uses the modulation technique proposed by (Jacobina et al., 2001), which are parameterized by μ. The homopolar voltage is then given by

$$v_{gk0}^* = v_{gk}^* + v_h \tag{6}$$

where,

$$v_h = v_{cc}(1/2-\mu)-(1-\mu)(max(v_{gk}^*))-\mu(min(v_{gk}^*)) \tag{7}$$

and $k = 1, 2, 3$. The model for dynamic control is obtained through the park transform of (2) to a synchronous reference frame (Rahmani et al., 2010). The dynamic model for control is given by

$$\frac{d}{dt}\begin{bmatrix} i_{gd} \\ i_{gq} \\ v_{cc} \end{bmatrix} = \begin{bmatrix} -\frac{R_{gf}}{L_{gf}} & \omega & -\frac{d_d}{L_{gf}} \\ -\omega & -\frac{R_{gf}}{L_{gf}} & -\frac{d_q}{L_{gf}} \\ \frac{d_d}{C} & \frac{d_q}{C} & 0 \end{bmatrix}\begin{bmatrix} i_{gd} \\ i_{gq} \\ v_{cc} \end{bmatrix} + \frac{1}{L_{gf}}\begin{bmatrix} e_{gd} \\ 0 \\ 0 \end{bmatrix} \tag{8}$$

where d_d and d_q is the control inputs (duty cycles of modulation). The system (8) is multiple-input multiple-output and nonlinear, what justifies the approach of this paper. For estimation of synchronization angle of grid is used the virtual flux calculation, which is defined by

$$\phi_{g\alpha\beta} = \int v_{g\alpha\beta}dt + L_{gf}i_{gf} \tag{9}$$

where $\alpha\beta$ corresponds to the axis of stationary reference frame (Clarke Transformation). A compensation of a constant has to be made to the angle obtained from (9), since it is 90° lagging the angles of voltage. A phase locked loop (PLL) is employed to reject harmonic frequencies and unbalance. More details of virtual flux can be obtained from (Malinowski et al., 2001; Malinowski, 2001).

2.1 Internal Control Loop

For development of control a nonlinear representation is adopted, given by

$$\begin{aligned} \frac{dX}{dt} &= F(x) + G(x)U \\ Y &= H(x) \end{aligned} \tag{10}$$

where

$$X = \begin{bmatrix} i_d \\ i_q \\ v_{cc} \end{bmatrix} \qquad F(x) = \begin{bmatrix} f_1(x) \\ f_2(x) \\ f_3(x) \end{bmatrix} = \begin{bmatrix} -\frac{R_{gf}}{L_{gf}}i_d + \omega i_q \\ -\omega i_d - \frac{R_{gf}}{L_{gf}}i_q \\ 0 \end{bmatrix}$$

$$G(x) = \begin{bmatrix} g_1(x) \\ g_2(x) \\ g_3(x) \end{bmatrix} = \begin{bmatrix} -\frac{v_{cc}}{L_{gf}} & 0 \\ 0 & -\frac{v_{cc}}{L_{gf}} \\ \frac{v_{cc}}{C} & \frac{v_{cc}}{C} \end{bmatrix}$$

$$U = \begin{bmatrix} d_d \\ d_q \end{bmatrix} \quad H(x) = \begin{bmatrix} i_d \\ i_q \end{bmatrix}$$

For the feedback linearization approach it is defined

$$\frac{dY}{dt} = \mathfrak{l}(x) + J(x)U = V \tag{11}$$

where

$$J(x) = \begin{bmatrix} \mathfrak{L}_{g1}(\mathfrak{L}_f^{r_1-1}(h_1)) & \mathfrak{L}_{g2}(\mathfrak{L}_f^{r_1-1}(h_1)) \\ \mathfrak{L}_{g1}(\mathfrak{L}_f^{r_2-1}(h_2)) & \mathfrak{L}_{g2}(\mathfrak{L}_f^{r_2-1}(h_2)) \end{bmatrix}$$

$$\mathfrak{l}(x) = \begin{bmatrix} \mathfrak{L}_f^{r_1}(h_1) \\ \mathfrak{L}_f^{r_2}(h_2) \end{bmatrix}$$

and

$$\frac{\partial h}{\partial x}f(x) = \mathfrak{L}_f h(x)$$

$$\frac{\partial h}{\partial x} g(x) = \mathfrak{L}_g h(x)$$

is called the Lie Derivative of h with respect to f or g, and r_k is the relative degree such that $\mathfrak{L}_g(\mathfrak{L}_f^{r_k-1}(h_k)) \neq 0$. So, for (10) is defined

$$\frac{d}{dt}\begin{bmatrix} i_d \\ i_q \end{bmatrix} = \begin{bmatrix} -\frac{R_{gf}}{L_{gf}} i_d + \omega i_q \\ -\omega i_d - \frac{R_{gf}}{L_{gf}} i_q \end{bmatrix} + \begin{bmatrix} -\frac{v_{cc}}{L_{gf}} & 0 \\ 0 & -\frac{v_{cc}}{L_{gf}} \end{bmatrix} \begin{bmatrix} d_d \\ d_q \end{bmatrix} \quad (12)$$

Then, the decoupled linear system can be obtained with the control law

$$U = J(x)^{-1}(V - \mathfrak{l}(x)) \quad (13)$$

or

$$\begin{bmatrix} d_d \\ d_q \end{bmatrix} = \begin{bmatrix} -\frac{L_{gf}}{v_{cc}} & 0 \\ 0 & -\frac{L_{gf}}{v_{cc}} \end{bmatrix} \left(\begin{bmatrix} v_d \\ v_q \end{bmatrix} - \begin{bmatrix} -\frac{R_{gf}}{L_{gf}} i_d + \omega i_q \\ -\omega i_d - \frac{R_{gf}}{L_{gf}} i_q \end{bmatrix} \right) \quad (14)$$

The controlled plant becomes

$$\frac{d}{dt}\begin{bmatrix} i_d \\ i_q \end{bmatrix} = \begin{bmatrix} v_d \\ v_q \end{bmatrix} \quad (15)$$

A state feedback can be used to allocate the poles of the system. For the tracking of constant components with null error an integral action is required. Thus, PID compensators are used. The control scheme in the Laplace domain is given by

$$s\begin{bmatrix} I_d \\ I_q \end{bmatrix} = \begin{bmatrix} -k_1 I_d + (K_p + K_i/s + K_d s)(I_d^* - I_d) \\ -k_1 I_q + (K_p + K_i/s + K_d s)(I_q^* - I_q) \end{bmatrix} \quad (16)$$

where K_p, K_i and K_d are the proportional, integral and derivative gains and I_d^* and I_q^* are the reference currents.

2.2 External Control Loop

As i_q should be zero due to the requirement of high power factor, the control of the bus must be performed by i_d. Furthermore,

$$p = e_{gd} i_{gd} \quad q = -e_{gd} i_{gq} \quad (17)$$

because $e_{gq} = 0$. For a variation of active power of the grid is obtained

$$\frac{dv_{cc}}{dt} = \frac{e_{gd} i_{gd}}{2 v_{cc} C} \quad (18)$$

where e_{gd} is the nominal value of the grid voltages. The nonlinear control eh given by

$$\frac{dy}{dt} = \mathfrak{L}_f h(x) + \mathfrak{L}_g h(x) u = \frac{e_{gd} i_{gd}}{2 v_{cc} C} \quad (19)$$

The control law is given by

$$u = \frac{1}{\mathfrak{L}_g \mathfrak{L}_f^{r_k-1} h(x)}(v - \mathfrak{L}_f^{r_k} h(x)) = i_{gd} = \frac{2 v_{cc} C}{e_{gd}} v \quad (20)$$

Table 1: Parameters from network, active filter and load.

Power Load	0.9kW (1 pu)
Power Load (Transients)	0.45kW (0.5 pu)
Line Voltage	110V (1pu)
Grid Frequency	60VHz
Bus Voltage	250V
Line Current	5A
Filter Inductance (L_f)	4mH
Inductor Resistance(R_f)	0.5 Ω
Grid Inductance(L_g)	3mH
Grid Resistance(R_g)	0.5 Ω
Switching Frequency	10Khz
Sampling	10Khz

A proportional feedback for pole allocation is used, and also a PI compensator to null tracking error for constant signals. The controlled system in the Laplace domain is given by

$$sV_{cc} = -k_c V_{cc} + (K_p + K_i/s)(V_{cc}^* - V_{cc}) \quad (21)$$

where k_c is the feedback gain for pole allocation and K_p and K_i are the proportional and integrative gain, respectively. The proposed control is shown in Fig. 2.

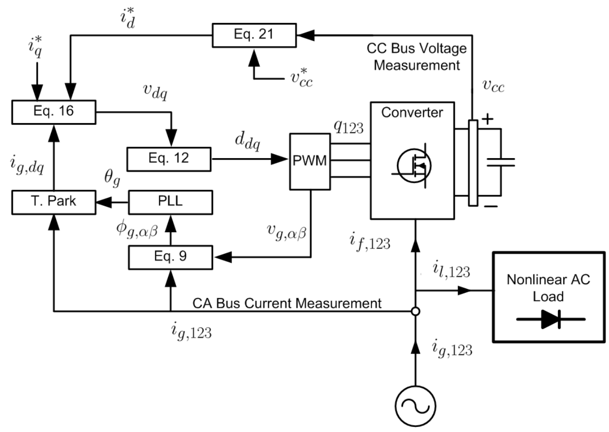

Figure 2: Proposed Nonlinear VFOC for Sensorless Active Filters.

3 SIMULATION AND EXPERIMENTAL RESULTS

For verification of the proposed controller, a simulation and experimental analysis was performed using a circuit with the parameters of Table 1. A three-phase diode rectifier is used as nonlinear load for compensation. The stationary results of simulation of the proposed control are shown in Fig 3. To validate the proposed control on transients, a load variation of 50% is performed and presented in Fig. 4. The transient instants are 0.5s (exit of load) and 0.7s (entrance of load). Fig.

DOI: 10.5540/03.2013.001.01.0024

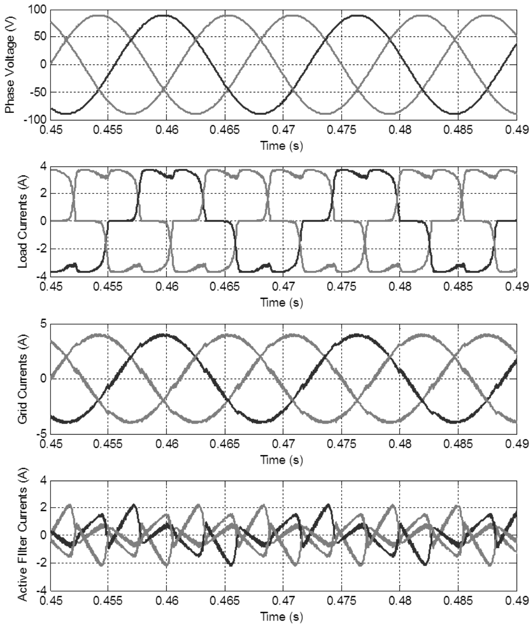

Figure 3: Simulation results. Stationary operation of sensorless active filter with the proposed controller.

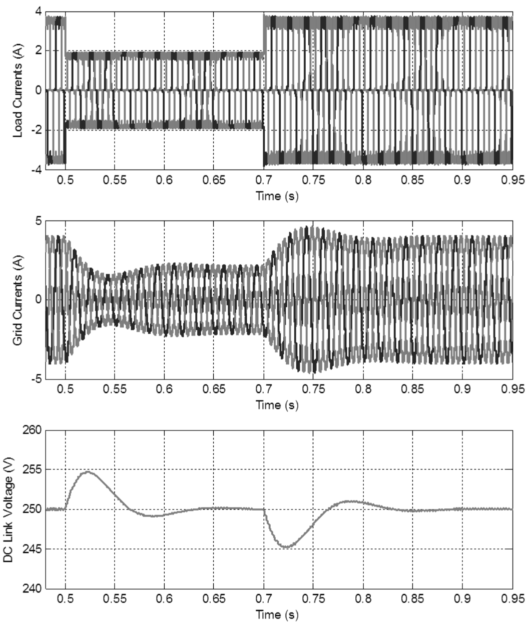

Figure 4: Simulation results. Transient operation of the sensorless active filter with the proposed controller. Load variation of 100% to 50%.

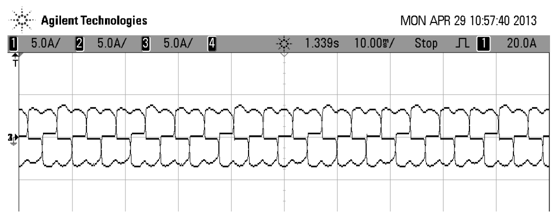

Figure 5: Experimental results. Load currents (6 pulse rectifier).

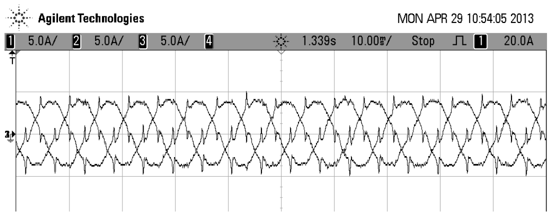

Figure 6: Experimental results. Grid currents with the proposed sensorless active filter.

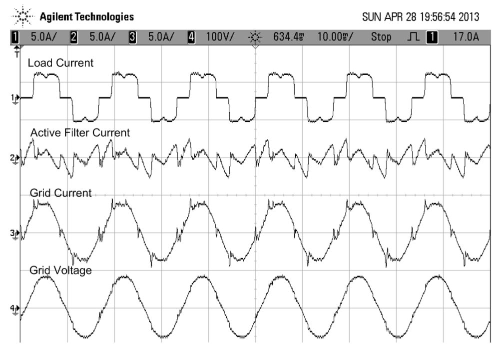

Figure 7: Experimental results. Currents and grid voltage, for phase 2, during the operation of the active filter with the proposed sensorless control.

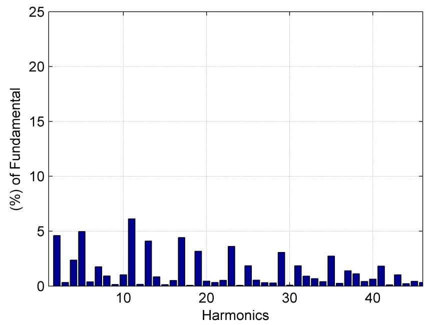

Figure 8: Experimental result. Harmonic analysis of grid currents. THD is 13%.

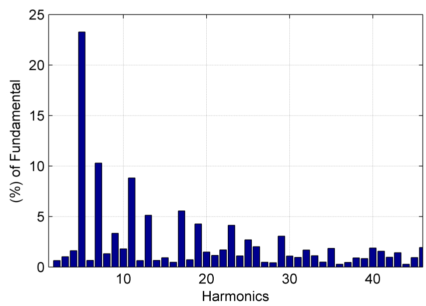

Figure 9: Experimental result. Harmonic analysis of load currents. THD is 28%.

DOI: 10.5540/03.2013.001.01.0024

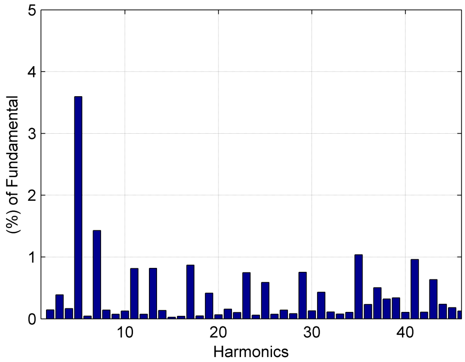

Figure 10: Experimental result. Harmonic analysis of grid voltage. THD is 5.1%

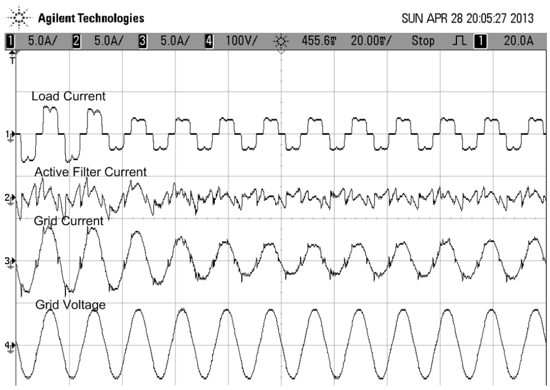

Figure 11: Experimental result. Transient operation of the sensorless active filter with the proposed controller. Load variation of 100% to 50%.

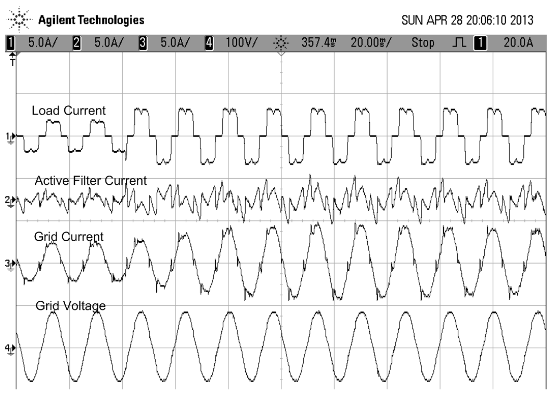

Figure 12: Experimental result. Transient operation of the sensorless active filter with the proposed controller. Load variation of 50% to 100%.

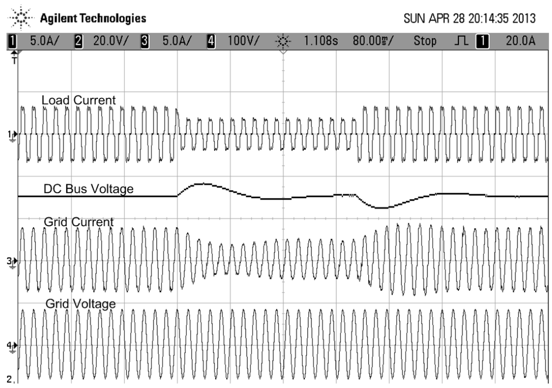

Figure 13: Experimental result. Transient operation of the sensorless active filter with the proposed controller. Load variation of 50%.

4 also shows the DC bus voltage during the transients.

The experimental analysis was performed through a prototype developed in the laboratory. The digital control was implemented in a computer, and the sensing was realized by means of analog/digital cards and hall effect sensors. Fig. 5 presents the experimental results of the nonlinear load employed, and Fig. 6 presents the experimental results of the grid currents for the active filter with the proposed control. Fig. 7 presents the experimental results of voltage and currents of phase 2 of the system.

The current THD of the nonlinear load is 28%, while the compensated currents of grid is 13%. The estimated power factor for stationary operation is 0.99. The harmonic analysis for load currents, grid current and voltage at coupling point are shown in Fig. 10, 8 and 9. As seen in the figures, the PID controllers allows to compensate the 5° and 7° harmonic of the nonlinear load, reducing to more than one quarter of the original magnitude.

A transient analyses is presented in Fig. 11. In this scenario there is a load removal of 50%. The transient of reinstitution to 100% of the original load is presented in Fig. 12. Fig. 13 presents the same transient together with the DC bus voltage. It was maximum variation of 6% with the reference in DC bus voltage.

4 CONCLUSION

This paper presents a control strategy applied to sensorless active filters using the feedback linearization approach. The control uses the concept of virtual flux to obtain the synchronization signals. As contributions , the present methodology is robust to variations of the operation points, and allows currents compensation of nonlinear loads with a reduced number of sensors, as well as treating multivariable interactions between dq loops.

Furthermore, the VFOC strategy allows compensation of the grid impedance, obtaining a high power factor operation, and consequently minimal grid current.

The proposed strategy has been validated in simulation and experimentally on a laboratory prototype. The stationary and transitory analysis was performed, and presented a stable and satisfactory operation of active filter.

ACKNOWLEDGEMENT

The authors acknowledge the financial support of CNPq.

References

Agirman, I. and Blasko, V. (2003). A novel control method of a vsc without ac line voltage sensors, *Industry Applications, IEEE Transactions on* **39**(2): 519–524.

Asiminoaei, A., Lascu, C., Blaabjerg, F. and Boldea, I. (2006). New current control structure for shunt active power filters, *Industry Applications Conference, 2006. 41st IAS Annual Meeting. Conference Record of the 2006 IEEE*, Vol. 1, pp. 183 –190.

Buso, S., Malesani, L. and Mattavelli, P. (1998). Comparison of current control techniques for active filter applications, *Industrial Electronics, IEEE Transactions on* **45**(5): 722–729.

Caceres, G., Lizarazo, J., Villalobos, M. and Suarez, J. (2010). Active power filters: A comparative analysis of current control techniques, *ANDESCON, 2010 IEEE*, pp. 1–6.

Cavini, A., Rossi, C., Tilli, A. and Tonielli, A. (2004). Digital implementation of decoupled nonlinear control strategies for shunt active filters, *Industrial Technology, 2004. IEEE ICIT '04. 2004 IEEE International Conference on*, Vol. 1, pp. 364–369 Vol. 1.

Hansen, S., Malinowski, M., Blaabjerg, F. and Kazmierkowski, M. (2000). Sensorless control strategies for pwm rectifier, *Applied Power Electronics Conference and Exposition, 2000. APEC 2000. Fifteenth Annual IEEE*, Vol. 2, pp. 832–838.

Jacobina, C., Nogueira Lima, A., da Silva, E., Alves, R. and Seixas, P. (2001). Digital scalar pulse-width modulation: a simple approach to introduce nonsinusoidal modulating waveforms, *Power Electronics, IEEE Transactions on* **16**(3): 351 –359.

Jiang, Z. and Xiang, L. (2012). Review of exact linearization method applied to power electronics system, *Power and Energy Engineering Conference (APPEEC), 2012 Asia-Pacific*, pp. 1–4.

Kennel, R. and Szczupak, P. (2005). Sensorless control of 3-phase pwm rectifier, *Industrial Electronics Society, 2005. IECON 2005. 31st Annual Conference of IEEE.*

Khadkikar, V. (2012). Enhancing electric power quality using upqc: A comprehensive overview, *Power Electronics, IEEE Transactions on* **27**(5): 2284–2297.

Malinowski, M. (2001). *Sensorless Control Strategies for Three-Phase PWM Rectifiers*, Ph.D. thesis, Warsaw Univerity of Techology, Faculty of Electrical Engineering, Warsaw - Poland.

Malinowski, M., Kazmierkowski, M., Hansen, S., Blaabjerg, F. and Marques, G. (2001). Virtual-flux-based direct power control of three-phase pwm rectifiers, *Industry Applications, IEEE Transactions on* **37**(4): 1019–1027.

Mendalek, N., Al-Haddad, K., Dessaint, L.-A. and Fnaiech, F. (2001). Nonlinear control strategy applied to a shunt active power filter, *Power Electronics Specialists Conference, 2001. PESC. 2001 IEEE 32nd Annual*, Vol. 4, pp. 1877–1882 vol. 4.

Noguchi, T., Tomiki, H., Kondo, S. and Takahashi, I. (1998). Direct power control of pwm converter without power-source voltage sensors, *Industry Applications, IEEE Transactions on* **34**(3): 473–479.

Rahmani, S., Mendalek, N. and Al-Haddad, K. (2010). Experimental design of a nonlinear control technique for three-phase shunt active power filter, *Industrial Electronics, IEEE Transactions on* **57**(10): 3364–3375.

Wojciechowski, D. (2005). Grid voltages sensorless control system of the pwm rectifier with active filtering function, *Compatibility in Power Electronics, 2005. IEEE*, pp. 238–246.

Yu, J. and peng Tang, Y. (2008). Ac current sensorless control of three-phase three-wire pwm rectifiers, *Intelligent Control and Automation, 2008. WCICA 2008. 7th World Congress on*, pp. 6516–6520.

DOI: 10.5540/03.2013.001.01.0024